

## Original Article

# Endoplasmic reticulum oxidoreductin 1 $\alpha$ mediates hepatic endoplasmic reticulum stress in homocysteine-induced atherosclerosis

Xiaoling Yang<sup>1†</sup>, Hua Xu<sup>1†</sup>, Yinju Hao<sup>2</sup>, Li Zhao<sup>3</sup>, Xin Cai<sup>3</sup>, Jue Tian<sup>1</sup>, Minghao Zhang<sup>1</sup>, Xuebo Han<sup>3</sup>, Shengchao Ma<sup>1</sup>, Jun Cao<sup>1</sup>, and Yideng Jiang<sup>1\*</sup>

<sup>1</sup>Department of Pathophysiology, Basic Medical School, Ningxia Medical University, Key Laboratory of Cardio-Cerebro-Vascular Diseases, Ningxia Medical University, Yinchuan 750004, China

<sup>2</sup>Department of Pharmacology, Ningxia Medical University, Yinchuan 750004, China

<sup>3</sup>Department of Clinical Examination, Ningxia Medical University, Yinchuan 750004, China

<sup>†</sup>These authors contributed equally to this work.

\*Correspondence address. Tel/Fax: +86-951-6980123; E-mail: yangwj04@126.com

**Endoplasmic reticulum (ER) stress is emerging as an important modulator of different pathological process and as a mechanism contributing to homocysteine (Hcy)-induced hepar injury. However, the molecular event that Hcy-induced ER stress in the hepar under the atherosclerosis background is currently unknown. Endoplasmic reticulum oxidoreductin 1 $\alpha$  (ERO1 $\alpha$ ) plays a crucial role in maintaining ER stress function. In this study, we determined the expression of ERO1 $\alpha$  in the hepar in hyperhomocysteinemia and the effect of ERO1 $\alpha$  in hepacytes ER stress in the presence of Hcy. HHcy model was established by feeding the methionine diet in apolipoprotein-E-deficient (ApoE<sup>-/-</sup>) mice, and the hepatocytes were incubated with folate and different concentrations of Hcy. Our results showed that Hcy triggered ER stress characterized by an increased contents of glucose-regulated protein 78 (GRP78), protein kinase RNA-like ER kinase (PERK), activating transcription factor (ATF) 6 and X-box binding protein-1 (XBP-1). The ERO1 $\alpha$  expressions in HHcy mice and Hcy-treated hepatocytes were decreased compared with those in ApoE<sup>-/-</sup> group and control hepacytes ( $P < 0.05$ ), respectively. Knocking-down the expression of ERO1 $\alpha$  with small-interfering RNA significantly augmented Hcy-induced ER stress. Meanwhile, the expressions of ER stress-related factor including GRP78, PERK, ATF6 and XBP-1, were significantly decreased when the ERO1 $\alpha$  gene was over-expressed in hepacytes. Our results suggested that ERO1 $\alpha$  may be involved in Hcy-induced hepar ER stress, and the inhibition of ERO1 $\alpha$  expression can accelerate this process.**

**Keywords** endoplasmic reticulum stress; endoplasmic reticulum oxidoreductin 1 $\alpha$ ; homocysteine; atherosclerosis

Received: April 13, 2014 Accepted: June 19, 2014

## Introduction

In eukaryotic cells, the endoplasmic reticulum (ER) is the site of protein transportation, folding, and assembly, and it involves lipid metabolism and steroid synthesis. Hypoxia, oxidative stress and hyperhomocysteinemia (HHcy) may induce physiological dysfunction of ER and trigger ER stress [1,2]. ER stress is a kind of cellular reaction for improving survival ability in harmful conditions by stimulating unfolded protein response (UPR) signal pathway. Adapted ER stress makes for protein renovating and boosts the ability to tolerate stress and stimulation, but severe and persistent ER stress has been regarded as a novel cell apoptosis signal besides death receptor activation and mitochondria injury [3]. When cells engage the ER stress, gene expression is modulated to promote either cell survival or apoptosis, depending on the nature, extent, and duration of the stress [4]. As a typical molecular pathophysiological process, ER stress is activated in many cardiovascular, endocrine, and hepatic diseases [5]. Hepatic cells contain abundant ER and are easy to trigger ER stress in the presence of various kinds of pathophysiological factor, and as a result, hepar lipid metabolism balance is broken and hepatic function is decreased.

HHcy has long been considered as an important independent risk factor of atherosclerosis (AS), which is accompanied by other organ injury during its development [6,7]. Increased homocysteine (Hcy) levels has been observed in experimental animal models of ethanol and CCl<sub>4</sub>-induced hepatotoxicity [8], and elevation of Hcy has also been found in patients with cirrhosis and chronic alcohol consumption [9]. Excessive superoxide anion that is generated by Hcy causes hepacyte oxidative stress and hepar injury [10]. Therefore, HHcy is involved in a wide range of impaired liver function. Hcy contains a free sulfhydryl group, which

can be oxidized with other thiols to form mixed disulfides. In this process, the sulfhydryl group is oxidized and reactive oxygen species (ROS) are generated. Consequently, the proteins are misfolded and ER stress occur [11]. When the misfolded proteins are formed, these proteins get through the ER membrane and trigger ER stress, consequently, hepar is impaired [11]. Hepar is the central organ in the synthesis and metabolism of lipoproteins and Hcy [12]. Hepar injury would affect the pathogenesis of AS [13]. To our knowledge, Hcy is involved in both AS and hepar ER stress. It is likely that Hcy-induced AS is closely related to hepar ER stress. Thus, alleviating hepar ER stress resulted from Hcy may be a better way to attenuate the development and progression of AS caused by HHcy. But up to now, the mechanism responsible for Hcy-induced liver ER stress, especially in AS background, is poorly understood.

ERO1 $\alpha$  that locates on human chromosome 14 and encodes a flavoprotein oxidase is identified as the primary oxidative source in the ER [14]. It promotes the formation of the disulfide bond in the unfolded protein and serves as a redox-sensor to maintain the proper oxidative environment of the ER [15]. Mammals have two genes which encode proteins homologous to ERO1 $\alpha$ , known as ERO1 $\alpha$  and ERO1 $\beta$  [16]. Wright and colleagues [17] have found that ERO1 $\alpha$  limits mutant proinsulin-induced ER stress. Modest inhibition of ERO1 $\alpha$  promotes signaling in the UPR and precondition cells against severe ER stress [18]. Therefore, ERO1 $\alpha$  is endowed with an important role for maintaining ER function and synthetic capacity. Because Hcy induces ER stress and UPR through disrupting disulfide bond formation and causing mis-folded proteins traversing the ER, we presume that ERO1 $\alpha$  is involved in Hcy-induced hepar ER stress during AS process.

Our previous study has shown that feeding apolipoprotein-E-deficient (ApoE $^{-/-}$ ) mice with a high methionine diet may induce HHcy, hypertriglyceridemia and AS [6]. In this study, we further observed the hepar ER stress during this process and tested the hypothesis that Hcy-induced hepar ER stress was mediated by down-regulation of ERO1 $\alpha$ .

## Materials and Methods

### Animal model

Male ApoE $^{-/-}$  mice (Animal Center of Peking University, Beijing, China) aged 6 weeks were divided into three groups ( $n = 10$  each): (1) hyperlipidaemia (HLA) group: mice were fed with regular mouse diet (0% cholesterol, 5.23% fat, 0.37% methionine, 2.39 mg/g choline, 3.19 mg/kg folate, 54.6  $\mu$ g/kg B12, 14.5 mg/kg B6); (2) HHcy group: mice were fed with regular mouse diet with 1.7% methionine supplement; (3) HHcy + folate + vitamin B12 group (HHcy + FA + VB) group: mice were fed with regular mouse diet plus 1.7% methionine, folate, and vitamin B12. Wild-type

C57BL/6J mice fed with regular mouse diet were used as control group. The animals were housed in a standard controlled animal care facility (six mice/cage) and were maintained in a temperature controlled room (22–25°C, 45% humidity) on a 12 : 12-h dark-light cycle for 15 weeks. The experimental procedures used on the mice were approved by the Ningxia Medical University Animal Care and Use Committee and was conducted according to the Ningxia Medical University Animal Care Committee guidelines.

### Electron microscopy

Conventional electron microscopy (EM) was performed as described [19]. In brief, hepar tissues were cut into  $\sim 1$  mm pieces, and placed immediately in 2.5% glutaraldehyde/1.5% paraformaldehyde solution at 4°C for 2 h. The pieces were post-fixed in 1% osmium tetroxide/1.5% potassium ferrocyanide solution. Then samples were dehydrated in ethanolacetone solution, and embedded in Epon 618. Afterwards, the epoxy blocks were sliced at 70–80 nm thickness and stained with uranyl acetate and lead citrate. All sections were observed with a Hitachi Hu-12A transmission electron microscope equipped with a Megaview III digital camera and Soft Imaging System (Olympus Corporation, Tokyo, Japan).

### Cell culture and homocysteine treatment

Mouse hepatocytes HL-7702 (Institute of Biochemistry and Cell Biology, Shanghai, China) were prepared and characterized as described previously [20]. In brief, hepatocytes were cultured in serum-free William's medium E (Gibco, Gaithersburg, USA), including 20 mU/ml insulin (Sigma, St Louis, USA), 50 ng/ml epidermal growth factor and fetal calf serum (FBS, Gibco). The medium was changed every two days. The aliquot cell suspensions were seeded into 24-well plates. After incubated with different concentrations (0, 50, 100, 200, 500  $\mu$ M) of Hcy (Sigma) and 30  $\mu$ M folate for 18 h, cells were collected for further use.

### Reverse transcription quantitative real-time polymerase chain reaction analysis

Total RNA from hepar tissues and hepatocytes were isolated using Trizol Reagent (Gibco) according to the manufacturer's instructions. First strand cDNAs were synthesized using SuperScript II reverse transcriptase (Promega, Southampton, UK). A reverse transcription quantitative real-time polymerase chain reaction (qRT-PCR) analysis was performed with the ABI Prism 7000 Sequence Detection System (Applied Biosystems, Foster City, USA) using SYBR<sup>®</sup> Premix-Ex Tag<sup>™</sup> (Takara, Dalian, China).  $\beta$ -actin was used as the internal control. A Ct value was obtained for each amplification curve and a  $\Delta$ Ct value was calculated by subtracting the Ct value for the corresponding internal control cDNA from the Ct value for each sample and transcript. Fold changes compared with the internal control were determined by calculating

the  $2^{-\Delta\Delta Ct}$ , and expression results are given as the expression ratio relative to  $\beta$ -actin.

### Western blot analysis

Hepar tissues and cells were lysed on ice for 30 min with lysis buffer (containing 0.15 M NaCl, 30 mM Tris, 1 mM phenylmethanesulfonyl fluoride, 1% Triton X-100, 1 mM EDTA, 10  $\mu$ g/ml leupeptin, 2  $\mu$ g/ml pepstatin, 2  $\mu$ g/ml aprotinin and 2 mM Na<sub>3</sub>VO<sub>4</sub>). Lysates containing equal amounts of protein (20–35  $\mu$ g, measured using BCA protein assay kit; Pierce, Rockford, USA) was mixed with 6  $\times$  sample buffer and then loaded on 10% sodium dodecyl sulfate polyacrylamide gel electrophoresis gels and blotted onto a PVDF membrane. After blocking with TBST plus 5% (w/v) dry non-fat milk, membranes were probed with primary antibodies (1 : 2000, anti-ERO1 $\alpha$ , anti-GRP78, anti-PERK, anti-ATF6 and anti-XBP-1; Sigma) overnight at 4°C. Subsequently, membranes were washed with TBST and probed with horseradish peroxidase conjugated anti-goat IgG secondary antibody (1 : 5000, Amersham Biosciences, Piscataway, USA) for 1 h at room temperature. After three times wash, the membranes were developed using an enhanced chemiluminescence detection kit (ECL Plus, Biyuntian, Shanghai, China). Band intensities were analyzed using a BioRad Gel Doc Imaging System with Quantity One software (BioRad, Hercules, USA) and normalized to the housekeeping band intensity ( $\beta$ -actin) on the same blot.

### Plasmid construction and transfection of ERO1 $\alpha$

The cDNA of ERO1 $\alpha$  gene was amplified using the primers 5'- CCGCTCGAGATGGGCCGCGGCTGGGGATTCTGT-3' (forward) and 5'-AATTCTGCAGATGAATATTCTGTAACAAGTTCCTGAAGTTTTTC-3' (reverse) and cloned into the vector pEGFP-N1 using the restriction sites *Xho*I and *Pst*I (underlined in the primer sequences). The amplified fragment was inserted in the *Xho*I/*Pst*I sites of pEGFP-N1 vector to create the recombinant plasmid, rp-ERO1 $\alpha$ . When hypocytes were in a subconfluent state, the recombinant plasmid was transiently transfected into cells using the polycationic lipid Roti-Fect (Roth, Lactan, Graz, Austria) or Lipofectamine 2000 Reagent (Invitrogen, Carlsbad, USA) according to the manufacturer's instructions. Twenty-four hours after transfection, cells were collected to determine the transfection efficiency by qRT-PCR and western blot analysis.

### siRNA silencing of ERO1 $\alpha$

Hepocytes were seeded at 70% confluence for siRNA transfection. siRNA targeting ERO1 $\alpha$  was composed of three different sequences (ON-TARGET plus set of 4 duplexes, Dharmacon, Beijing, China) that match different parts of ERO1 $\alpha$  mRNAs. The purpose of using three different siRNA sequences for a target gene was to cut down target

effects and keep high silencing potency. The final concentration of used siRNAs was 100 nM, and siRNA transfection was performed in accordance with Lipofectamine 2000 introductions. Nucleotide sequences of siRNA are listed below: ERO1 $\alpha$ -689 (siRNA1): (sense) 5'-GACCAAGCAUGAUGAUUCUTT-3', (anti-sense) 5'-AGAAUCAUCAUGC UUGGUUCTT-3'; ERO1 $\alpha$ -436 (siRNA2): (sense) 5'-GUGACUACUUUAGGUAUUATT-3', (anti-sense) 5'-UAAUACC UAAAGUAGUACTTA-3'; ERO1 $\alpha$ -958 (siRNA3): (sense) 5'-GAGCAUUCUACAGACUUUATT-3', (anti-sense) 5'-AUAAGUCUGUAGAAUGCUCTT-3'. Silencer negative control FAM siRNA (sense 5'-UUCUCCGAACGUGUCACGUTT-3', anti-sense: 5'-ACGUGACACGUUCGGAGAATT-3') was used as control. After overnight transfection, medium was substituted with complete William's medium E medium containing 10% FBS & 1% penicillin/streptomycin. The cells were cultured for 48 h until further use. Knockdown efficiency was examined by qRT-PCR or western blot analysis.

### Statistical analysis

The data were shown as mean  $\pm$  standard error of the mean (SEM). For the comparisons among the experimental groups, when data presented a normal distribution and variance homogeneity, one-way analysis of variance and additional analysis of variance test were used. Otherwise, the corresponding nonparametric test was used. Statistical analysis was performed using Microsoft Excel spreadsheets and SPSS 13.0 for Windows.  $P < 0.05$  was considered statistically significant.

## Results

### HHcy induced hepar ER structure change

To evaluate whether HHcy led to serious ER stress in hepar, we used the scanning EM to observe the cell morphology. The results showed that in the hepar ER of HLA group, there were slight pathological lesions characterized by hyperplasia and irregular arrangement of rough ER, reducing the number of smooth ER (**Fig. 1A,B**). In the HHcy group, we found an obvious swell and degranulation of rough ER, expansion of ER lumen, formation of vacuole and eclasis of ribosome from rough ER (**Fig. 1C**). In the HHcy + FA + VB group (**Fig. 1D**), although rough ER hypertrophy was observed, these pathological damages were lighter than those of HHcy group, while the control group displayed a consistent and compact structure, with the ribosome on the ER. These results indicated that HHcy may aggravate the pathological damage of hepar ER in ApoE $^{-/-}$  mice.

### HHcy promoted hepar ER stress

Because glucose-regulated protein 78 (GRP78) is one of the ER chaperones and is an important molecular marker of ER

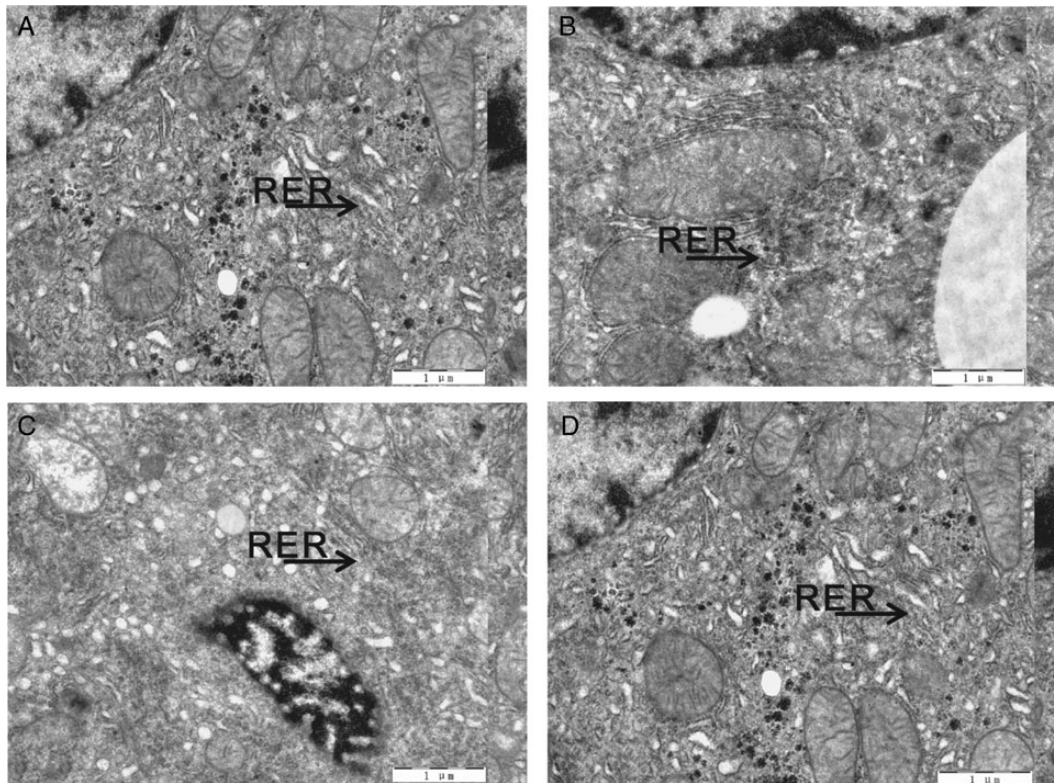


**Figure 1. The morphological changes of endoplasmic reticulum in mice of each group** Representative electron microscopy shows normal ultrastructure in control (A), HLA (B), HHcy (C), or HLA + FA + VB group (D) ( $n = 10$ /group). Arrows show hyperplasia of rough endoplasmic reticulum (RER) in hepatocyte image ( $\times 3000$ ).

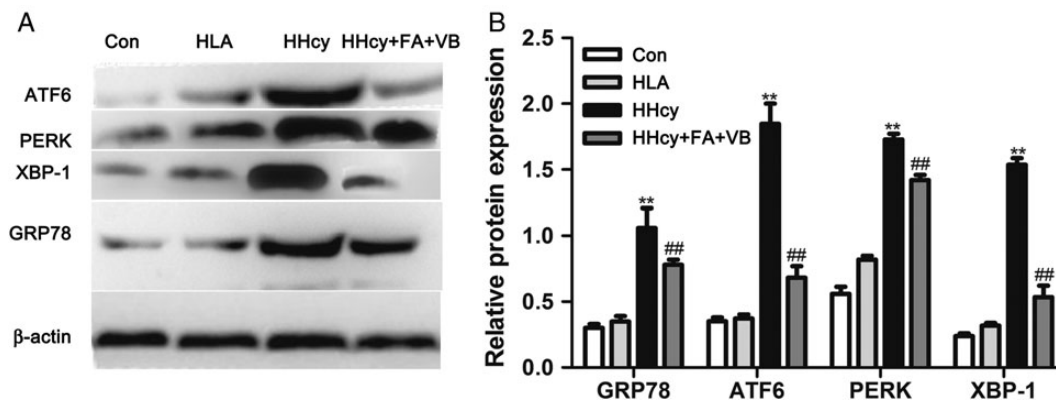


**Figure 2. Expressions of GRP78, ATF6, PERK, XBP1 in the hepar of mice** 15 weeks later, mice were killed and the hepar tissues were collected and lysated for determining the expression of GRP78, ATF6, PERK, and XBP1 by western blot analysis. Data were expressed as mean  $\pm$  SEM ( $n = 10$ ). \*\* $P < 0.01$  vs. Con and HLA; ## $P < 0.01$  vs. HHcy.

stress, we further detect the expression of GRP78 in hepar by western blot analysis. Our results showed that the expression of GRP78 was increased to 2-fold times in the HHcy group when compared with the control and HLA groups, respectively. The expression of GRP78 in HHcy + FA + VB group was lower compared with that in HHcy group. There was no significant difference between the control and HLA groups. Morphological changes and a significant increase of GRP78 expression indicated aggravating ER stress in hepar from HHcy-induced AS (Fig. 2).

Protein kinase RNA-like ER kinase (PERK), activating transcription factor (ATF) 6 and X-box binding protein-1 (XBP-1) are three downstream targets of GRP78. In order to further confirm HHcy-induced ER stress, we then detected the expressions of these three ER stress protein in hepar. We found that ATF6 level in HHcy group was significantly elevated when compared with that in the control and HLA group. ATF6 level in HHcy + FA + VB group was lower than that in HHcy group ( $P < 0.01$ , Fig. 2). Consistent with the result from ATF6, levels of XBP-1 and PERK in HHcy

group were higher than that in HLA group, respectively. In HHcy + FA + VB group, XBP-1 and PERK levels were lowered as compared with the HHcy group ( $P < 0.01$ ). However, there were no significant differences of PERK, XBP-1, and ATF6 between the control and HLA group ( $P > 0.05$ , **Fig. 2**). These results indicated that these three downstream signals were involved in hepatic ER stress in HHcy-induced AS.

**ERO1 $\alpha$  expressions were up-regulated in hepatic**

*ERO1 $\alpha$*  is a key gene in UPR and formation of disulfide bonds and is closely related to ER stress. We then observed the expression of *ERO1 $\alpha$*  in hepatic in HHcy-induced AS. **Figure 3** showed that the relative mRNA and protein expression of *ERO1 $\alpha$*  in HLA group were decreased by 23.38% and 16.08% when compared with the control group ( $P < 0.01$ , **Fig. 3A,B**). In HHcy group, the mRNA and protein

expression of *ERO1 $\alpha$*  was decreased by 73.35% and 33.03% as compared with the HLA group. In HHcy + FA + VB group, *ERO1 $\alpha$*  mRNA and protein expression was 96.42% and 29.03% more than that in the HHcy group ( $P < 0.01$ , **Fig. 3A,B**). Our findings suggested that *ERO1 $\alpha$*  expression in hepatic was decreased at both transcriptional and translational level in HHcy-induced AS.

**Hcy induced down-regulation of *ERO1 $\alpha$*  expression in hepatic**

We also investigated the mRNA and protein expression levels of *ERO1 $\alpha$*  in hepatic in the presence of Hcy. Consistent with the results from the mice, *ERO1 $\alpha$*  expressions in hepatic were substantially down-regulated after incubation with Hcy at various doses (50, 100, 200 and 500  $\mu$ M) in a dose-dependent manner (**Fig. 4A,B**). After folate and vitamin B12 treatment, *ERO1 $\alpha$*  mRNA

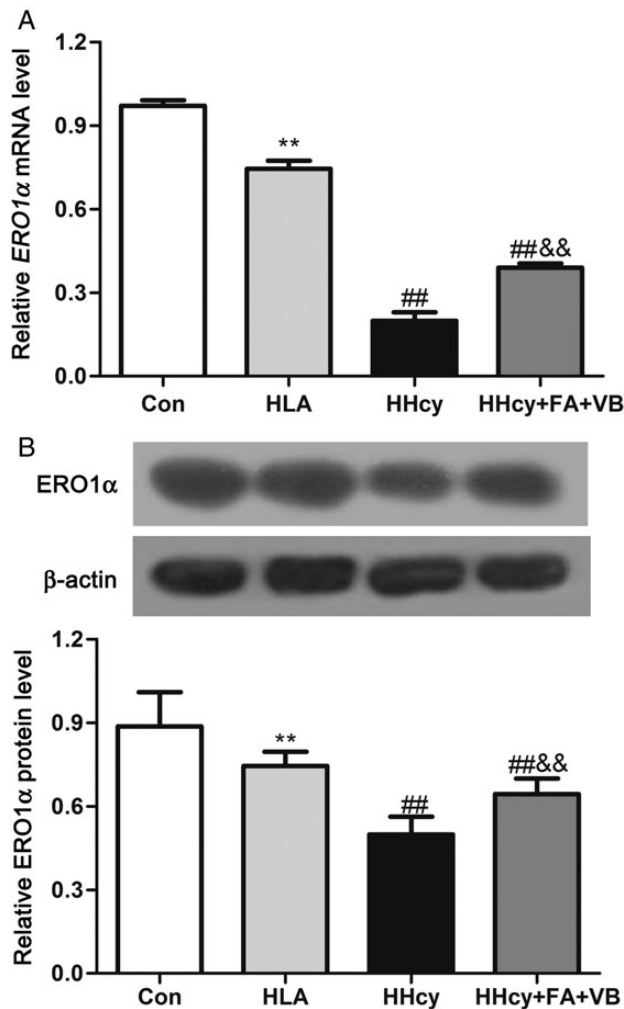


**Figure 3. *ERO1 $\alpha$*  mRNA and protein expressions in the hepatic of mice** Total RNA and protein in the hepatic tissues were extracted. *ERO1 $\alpha$*  mRNA (A) and protein (B) expression were detected by qRT-PCR and western blot analysis. Data were expressed as mean  $\pm$  SEM ( $n = 10$ ). \*\* $P < 0.01$  vs. Con; ### $P < 0.01$  vs. HLA; && $P < 0.01$  vs. HHcy.

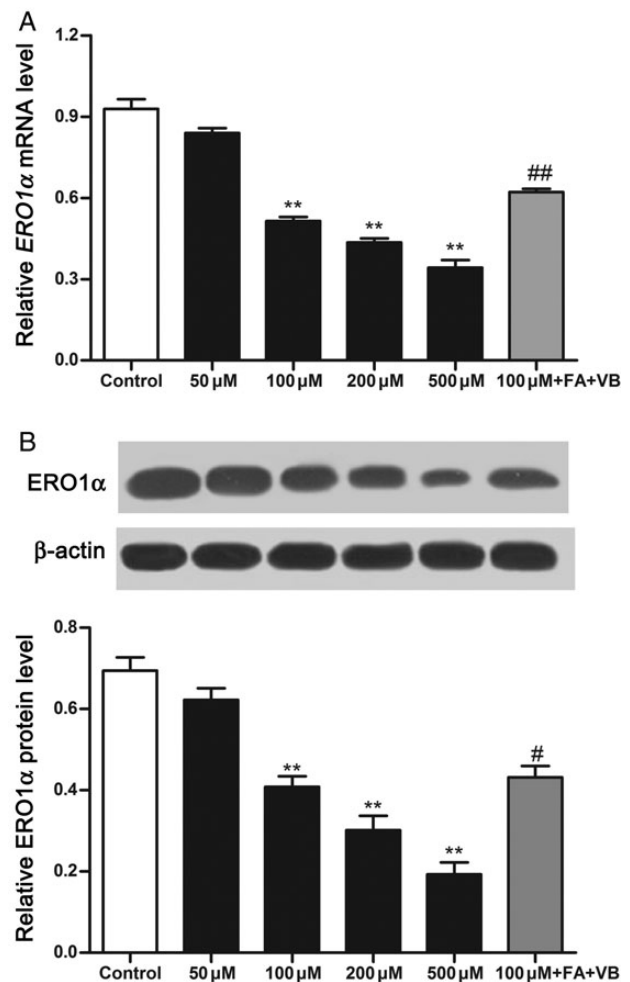


**Figure 4. Effects of Hcy on *ERO1 $\alpha$*  expression in hepatic** After cells were treated with Hcy for 24 h, *ERO1 $\alpha$*  mRNA (A) and protein expression (B) in hepatic were detected by qRT-PCR and western blot analysis. Data were expressed as mean  $\pm$  SEM. \*\* $P < 0.01$  vs. Con; # $P < 0.05$  vs. 100  $\mu$ M Hcy; ### $P < 0.01$  vs. 100  $\mu$ M Hcy.

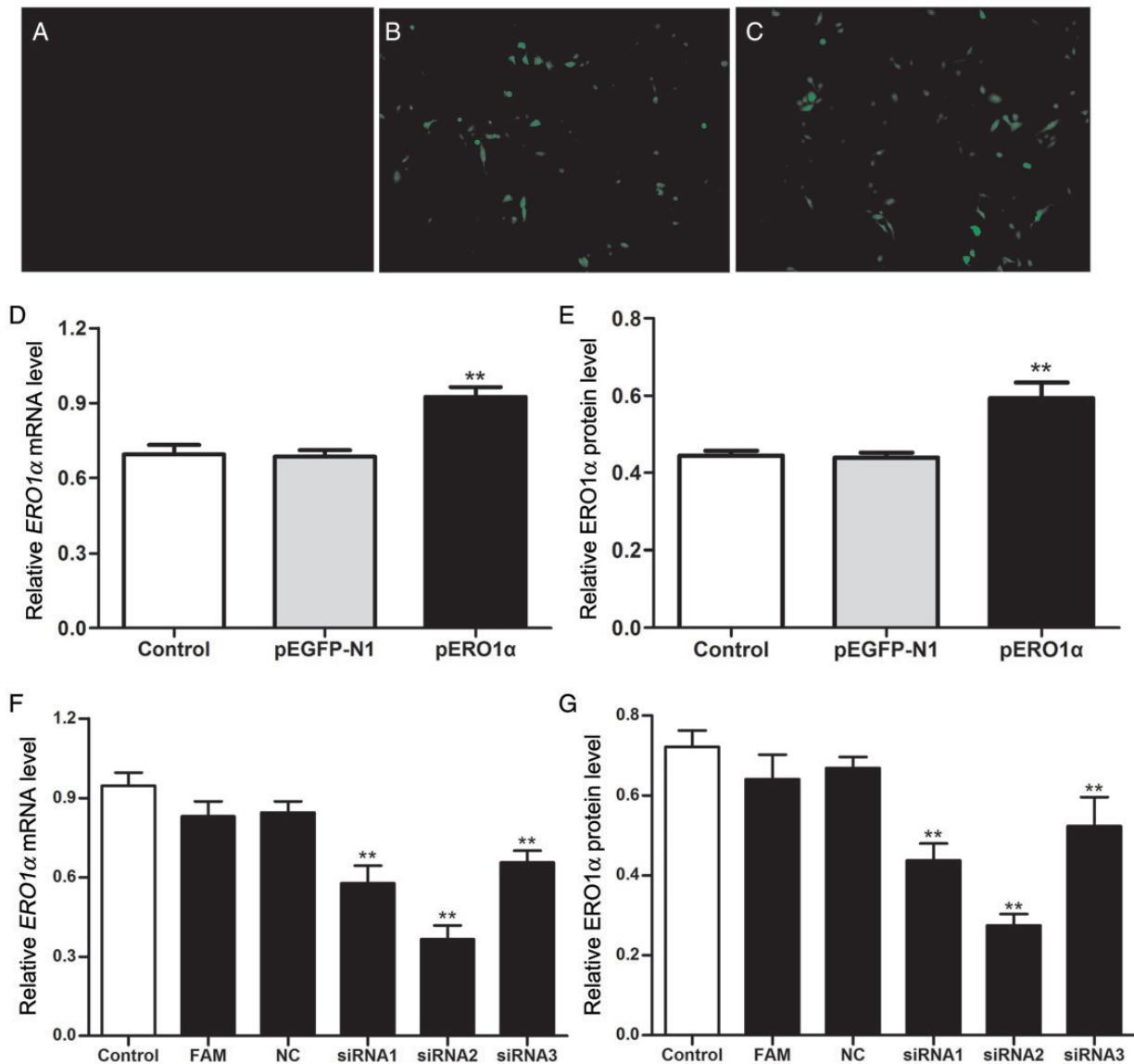


**Figure 5. ERO1 $\alpha$  expression in hepacytes** When cells were in logarithmic growth phase, pEGFP-N1 plasmid which carried *ERO1 $\alpha$*  cDNA was transfected into hepacytes, and the expression of fluorescence intensity (A, B, C), mRNA (D) and protein (E) were determined by fluorescence microscopy, qRT-PCR, and western blot analysis. Meanwhile, siRNA fragments were also transfected into hepacytes to detect the *ERO1 $\alpha$*  mRNA (F), protein (G) expression. Data were expressed as mean  $\pm$  SEM. \*\* $P < 0.01$  vs. control.

expressions were 20.73% more than that of 100  $\mu$ M Hcy. The effect of Hcy on the protein levels of ERO1 $\alpha$  in hepacytes was similar to its effect on mRNA expression. Protein level of ERO1 $\alpha$  in 100, 200, and 500  $\mu$ M Hcy groups were decreased by 41.19%, 56.51%, and 72.22% when compared with that in the control group ( $P < 0.01$ ), respectively. Folate and vitamin B12 also affected ERO1 $\alpha$  protein expression in the presence of Hcy. We found that the relative expression of ERO1 $\alpha$  in 100  $\mu$ M + FA + VB group were increased by 5.81% compared with the 100  $\mu$ M Hcy group ( $P < 0.05$ , Fig. 4A,B). These results indicated that Hcy affected the expression of ERO1 $\alpha$  at both transcriptional and translational levels in hepacytes.

#### Effect of ERO1 $\alpha$ on Hcy-induced ER stress

In order to determine the exact function of ERO1 $\alpha$  in hepacytes, we over-expressed *ERO1 $\alpha$*  gene in hepacytes. *ERO1 $\alpha$*  cDNA was introduced into the HL-7702 cells using pEGFP-N1 plasmid that carried an enhanced green fluorescence protein (EGFP). Then we observed an obvious expression of green fluorescent in the transfected cells, but no fluorescence was found in the control (Fig. 5A–C). We found that mRNA expressions of ERO1 $\alpha$  were significantly increased by 33.22% and 34.88% in recombinant plasmid group compared with the control and blank vector groups ( $P < 0.01$ , Fig. 5D). In blank vector group, there was no significant difference of ERO1 $\alpha$  expression either at

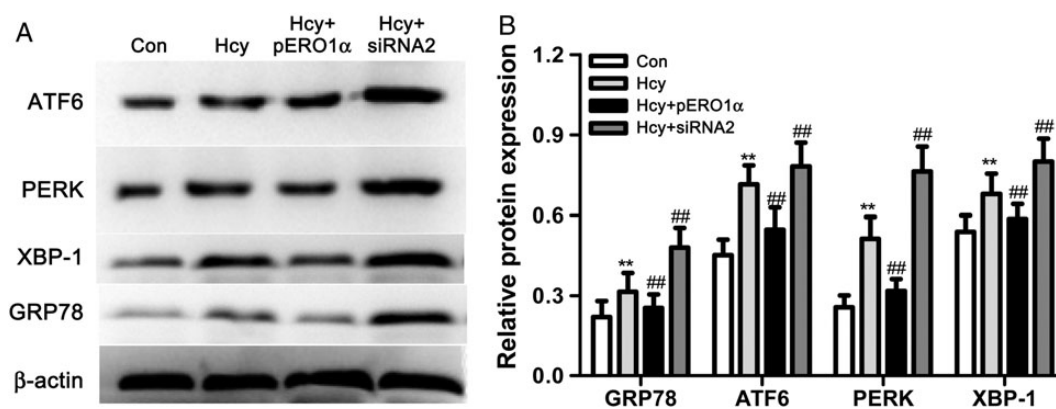


**Figure 6. Involvement of ERO1 $\alpha$  in Hcy-induced ERS** After cells were transfected with p-ERO1 $\alpha$  and si-ERO1 $\alpha$ , Hcy was added, protein levels of ERS related factor including GRP78, ATF6, PERK, and XBP-1 were assayed by western blot analysis. Data were expressed as mean  $\pm$  SEM. \*\* $P$  < 0.01 vs. control; ## $P$  < 0.01 vs. Hcy.

transcriptional or at translational level compared with the control. Consistent with the result from mRNA, the protein expression of ERO1 $\alpha$  in recombinant plasmid group was also increased by 33.55% and 35.13% compared with the control and blank vector groups (Fig. 5E). In addition, three siRNAs were transfected into hepatocytes. As expected, ERO1 $\alpha$  expression was blocked after siRNAs incubation. mRNA expression in hepatocytes were decreased by  $\sim$ 38.94% ( $P$  < 0.01), 61.30% and 30.59% for siRNA1, siRNA2, and siRNA3, respectively (Fig. 5F). Similarly, its protein expression also decreased by 39.38%, 61.88%, and 27.47% for siRNA1, siRNA2, and siRNA3, respectively ( $P$  < 0.01, Fig. 5G). Because the interfering effect of siRNA2 on ERO1 $\alpha$  expression was the highest among these three siRNAs, we chosen siRNA2 for further study.

We then observed the effects of ERO1 $\alpha$  in hepatocytes ER stress in the presence of Hcy. Consistent with results from *in vivo* experiment, after Hcy incubation, GRP8, ATF6, PERK, and XBP-1 were increased by 1.43, 1.58, 2.00, and 1.26-folds compared with the control group. Over-expression of ERO1 $\alpha$  in hepatocytes in the presence of Hcy resulted in 19.36%, 23.53%, 38.14%, and 13.55% decrease of GRP78, ATF6, PERK, and XBP-1, respectively, when compared with Hcy incubation alone, meanwhile, knockdown of ERO1 $\alpha$  by siRNA2 resulted in 1.52, 1.09, 1.49, and 1.18-folds increase in the levels of GRP78, ATF6, PERK, and XBP-1, as compared with the Hcy group ( $P$  < 0.01, Fig. 6). These results indicated that ERO1 $\alpha$  might restrain ER stress and it might be a key factor in Hcy-induced hepatocytes ER stress.

## Discussion

In this study, we demonstrated the involvement of ERO1 $\alpha$  in Hcy-induced ER stress both *in vivo* and *in vitro*. In ApoE $^{-/-}$  mice, HHcy induced hepar ER stress which was characterized by the activation of GRP78, ATF6, XBP-1, and PERK, and ER stress could be attenuated by folate and vitamin B12.

After exposure to Hcy, ER stress-related factors were also activated, while folate and vitamin B12 contributed to relieve this process in hepatocytes. Over-expression or knock-down of ERO1 $\alpha$  in hepatocytes also induced changes of ER stress-related factors contents. These results proved for the first time that Hcy-induced ER stress in hepatocytes is mediated, at least in part, by ERO1 $\alpha$ .

Hepar is a major metabolic organ of Hcy. Evidence has shown that chronic ethanol administration alters methionine in the liver, resulting in Hcy release into the plasma. Our previous study also proved that serum Hcy levels were significantly increased in ApoE $^{-/-}$  mice after feeding with high methionine diet [6]. An excess of Hcy may promoted UPR and induce accumulation of misfolded proteins under ER stress [21]. Wei *et al.* [22] also reported that methionine overload induced HHcy and caused a marked ER stress. Transcriptional activation of ER chaperone protein is the marker of ER stress, and GRP78 is the typical one that binds to ATF6, PERK, and IRE1 in normal condition [23]. When the cells are under stress, these transmembrane transducers will be separated from GRP78 and activate downstream signal pathway to initiate UPR [24]. Activation of PERK causes phosphorylation of the eukaryotic translation initiation factor 2 $\alpha$  and then inhibits protein synthesis. Activated IRE1 catalyzes the removal of a small intron from the XBP-1 mRNA, which triggers the induction of ER chaperones and other genes involved in ER-associated protein degradation [23]. ATF6 and XBP-1 may combine to the ER stress response element and the UPR element, leading to GRP78 expression [25]. Our results showed that the expressions of GRP78, ATF6, XBP-1, and PERK in hepar were increased in HHcy group. By using the EM, we also found a severe swell and degranulation of rough ER, expansion of ER lumen. Moreover, in our *in vitro* experiment, we also found the increased expressions of ER stress-related proteins including GRP78, ATF6, XBP-1, and PERK in the presence of Hcy. So we concluded that Hcy might induce hepar ER stress in AS background and it might be a strong activator of ER stress.

ERO1 $\alpha$  plays an essential role in maintaining the redox potential in the ER, and the regulation of ERO1 $\alpha$  activity is the central to keep redox homeostasis and proper ER folding activity [26]. Dysfunction of ERO1 $\alpha$  leads to a rapid decline in oxidative protein folding, strong activation of the UPR, and potential source of ER-derived oxidative stress [27]. In the mammalian ER, ERO1 $\alpha$  oxidized PDI, which, in turn, introduces disulfides into ER-related proteins to trigger UPR [15]. Specific and limited PDI oxidation by ERO1 $\alpha$  is essential to avoid ER hyperoxidation [28]. A study has shown the increased transient protein expression levels in Chinese hamster ovary cells engineered to express ERO1 $\alpha$  [29]. Lowered levels of ERO1 $\alpha$  can protect prokaryocyte and cultured eukaryotic cells against severe ER stress [18]. Here, we showed that ERO1 $\alpha$  levels were increased in HHcy mice liver, which was consistent with that ERO1 $\alpha$  expression in mice were up-regulated during a much later stage of tunicamycin-induced stress response [28]. Meanwhile, we also observed a similar result of ERO1 $\alpha$  expression in hepacytes after Hcy stimulation. When the cells were treated with vitamin B12 and folic acid, a recovery of ERO1 $\alpha$  expression was observed. These data indicated that Hcy promoted the expression of ERO1 $\alpha$  both *in vivo* and *in vitro*.

Over-expression of ERO1 $\alpha$  has been shown to induce a significant increase in ROS, whereas lowering of ERO1 $\alpha$  level by RNAi enhanced resistance to the lethal effects of high levels of ER stress [30]. Moreover, the combined elevation of ERO1 $\alpha$  with an increased ER client protein load can have lethal consequences [28]. In order to explicitly analyze the exact effect of ERO1 $\alpha$  in Hcy-induced ER stress, we further over-expressed *ERO1 $\alpha$*  gene or knockdown this gene in hepacytes to detect the ER stress. Our results revealed that, in the presence of Hcy, ER stress reaction was strengthened when transcriptional activation of ERO1 $\alpha$  was boosted in hepacytes. In contrast, contents of ER stress-related protein were decreased in the ERO1 $\alpha$  knockdown cells. Vitamin B12 and folic acid contributed to alleviate Hcy-induced ER stress in ERO1 $\alpha$  transfected hepacytes. As one of the traditional metabolic pathways of Hcy is transsulfenyl, and ERO1 $\alpha$  has the ability to form disulfide bond, we proposed that Hcy may transfer sulfhydryl group to other substance such as ERO1 $\alpha$  to cause ER stress, which might be a novel mechanism for Hcy to induce AS, which needs to be further explored.

In conclusion, these data demonstrated a definite role for ERO1 $\alpha$  in promoting ER stress in the presence of Hcy, and suggested that ERO1 $\alpha$  may mediate the effects of metabolic perturbations in Hcy-induced AS. This finding would provide a novel strategies in clinical treatment of AS. However, the underlying mechanism of ERO1 $\alpha$  in Hcy-induced liver ER stress is still not clear, which will be the focus of our further study.

## Acknowledgements

We would like to thank Prof. Wei Zhao and Yan Zhang for their assistance in electron microscopy. We also thank Prof. Yunhong Li for his help in the immunofluorescence experiment.

## Funding

This work was supported in part by grants from the National Natural Science Foundation of China (81360073, 81260063, 81360027), and the Provincial Natural Science Foundation of Ningxia (NZ13054, NZ12174).

## References

- Li Y, Zhang H, Jiang C, Xu M, Pang Y, Feng J and Xiang X, *et al.* Hyperhomocysteinemia promotes insulin resistance by inducing endoplasmic reticulum stress in adipose tissue. *J Biol Chem* 2013, 288: 9583–9592.
- Liu H, Zhao S, Zhang Y, Wu J, Peng H, Fan J and Liao J, *et al.* Reactive oxygen species-mediated endoplasmic reticulum stress and mitochondrial dysfunction contribute to polydatin-induced apoptosis in human nasopharyngeal carcinoma CNE cells. *J Cell Biochem* 2011, 112: 3695–3703.
- Wang C, Jiang K, Gao D, Kang X, Sun C, Zhang Q and Li Y, *et al.* Clusterin protects hepatocellular carcinoma cells from endoplasmic reticulum stress induced apoptosis through GRP78. *PLoS One* 2013, 8: e55981.
- Logue SE, Cleary P, Saveljeva S and Samali A. New directions in ER stress-induced cell death. *Apoptosis* 2013, 8: 537–546.
- Cao SS and Kaufman RJ. Targeting endoplasmic reticulum stress in metabolic disease. *Expert Opin Ther Targets* 2013, 17: 437–448.
- Jiang Y, Zhang H, Sun T, Wang J, Sun W, Gong H and Yang B, *et al.* The comprehensive effects of hyperlipidemia and hyperhomocysteinemia on pathogenesis of atherosclerosis and DNA hypomethylation in ApoE<sup>-/-</sup> mice. *Acta Biochim Biophys Sin* 2012, 44: 866–875.
- Schramm R, Appel F, Reinacher M, Schafers HJ, Bierbach B, Slotta J and Thorlacius H, *et al.* Atherosclerosis aggravates ischemia/reperfusion injury in the gut and remote damage in the liver and the lung. *Inflamm Res* 2011, 60: 555–567.
- McClain C, Barve S, Joshi-Barve S, Song Z, Deaciuc I, Chen T and Hill D. Dysregulated cytokine metabolism, altered hepatic methionine metabolism and proteasome dysfunction in alcoholic liver disease. *Alcohol Clin Exp Res* 2005, 29: 180S–188S.
- Sakuta H and Suzuki T. Alcohol consumption and plasma homocysteine. *Alcohol* 2005, 37: 73–77.
- Matte C, Stefanello FM, Mackedanz V, Pederzoli CD, Lamers ML, Dutra-Filho CS and Dos Santos MF, *et al.* Homocysteine induces oxidative stress, inflammatory infiltration, fibrosis and reduces glycogen/glycoprotein content in liver of rats. *Int J Dev Neurosci* 2009, 27: 337–344.
- Elanchezian R, Palsamy P, Madson CJ, Lynch DW and Shinohara T. Age-related cataracts: homocysteine coupled endoplasmic reticulum stress and suppression of Nrf2-dependent antioxidant protection. *Chem Biol Interact* 2012, 200: 1–10.
- Hunt CE, Diani AR, Brown PK, Kaluzny MA and Epps DE. Diet induced atherogenic hyperlipoproteinaemia and liver injury in cynomolgus macaques. *Br J Exp Pathol* 1986, 67: 235–249.
- Boddi M, Tarquini R, Chiostrì M, Marra F, Valente S, Giglioli C and Gensini GF, *et al.* Nonalcoholic fatty liver in nondiabetic patients with acute coronary syndromes. *Eur J Clin Invest* 2013, 43: 429–438.



14. Araki K and Inaba K. Structure, mechanism, and evolution of Ero1 family enzymes. *Antioxid Redox Signal* 2012, 16: 790–799.
15. Inaba K, Masui S, Iida H, Vavassori S, Sitia R and Suzuki M. Crystal structures of human Ero1 $\alpha$  reveal the mechanisms of regulated and targeted oxidation of PDI. *EMBO J* 2010, 29: 3330–3343.
16. Chin KT, Kang G, Qu J, Gardner LB, Coetzee WA, Zito E and Fishman GI, *et al.* The sarcoplasmic reticulum luminal thiol oxidase ERO1 regulates cardiomyocyte excitation-coupled calcium release and response to hemodynamic load. *FASEB J* 2011, 25: 2583–2591.
17. Wright J, Birk J, Haataja L, Liu M, Ramming T, Weiss MA and Appenzeller-Herzog C, *et al.* Endoplasmic reticulum oxidoreductin-1 $\alpha$  (Ero1 $\alpha$ ) improves folding and secretion of mutant proinsulin and limits mutant proinsulin-induced ER stress. *J Biol Chem* 2013, 288: 31010–31018.
18. Blais JD, Chin KT, Zito E, Zhang Y, Heldman N, Harding HP and Fass D, *et al.* A small molecule inhibitor of endoplasmic reticulum oxidation 1 (ERO1) with selectively reversible thiol reactivity. *J Biol Chem* 2010, 285: 20993–21003.
19. Mogilnaya O, Puzyr A, Baron A and Bondar V. Hematological parameters and the state of liver cells of rats after oral administration of aflatoxin b1 alone and together with nanodiamonds. *Nanoscale Res Lett* 2010, 5: 908–912.
20. Zhen A, Qi YM, Huang DJ, Gu XY, Tian YH, Li P and Li H, *et al.* EGCG inhibits Cd<sup>(2+)</sup>-induced apoptosis through scavenging ROS rather than chelating Cd<sup>(2+)</sup> in HL-7702 cells. *Toxicol Mech Methods* 2014, 4: 259–267.
21. Ignashkova TI, Mesitov MV, Rybakov AS, Moskovtsev AA, Sokolovskaia AA and Kubatiev AA. Deposition of von Willebrand factor in human endothelial cells HUVEC in the endoplasmic reticulum stress induced by an excess of homocysteine *in vitro*. *Patol Fiziol Eksp Ter* 2012, 3: 81–86.
22. Wei H, Zhang R, Jin H, Liu D, Tang X, Tang C and Du J, *et al.* Hydrogen sulfide attenuates hyperhomocysteinemia-induced cardiomyocyte endoplasmic reticulum stress in rats. *Antioxid Redox Signal* 2010, 12: 1079–1091.
23. Wolfson JJ, May KL, Thorpe CM, Jandhyala DM, Paton JC and Paton AW. Subtilase cytotoxin activates PERK, IRE1 and ATF6 endoplasmic reticulum stress-signalling pathways. *Cell Microbiol* 2008, 10: 1775–1786.
24. Malhi H and Kaufman RJ. Endoplasmic reticulum stress in liver disease. *J Hepatol* 2011, 54: 795–809.
25. Nozaki Ji, Kubota H, Yoshida H, Naitoh M, Goji J, Yoshinaga T and Mori K, *et al.* The endoplasmic reticulum stress response is stimulated through the continuous activation of transcription factors ATF6 and XBP1 in Ins2+/Akita pancreatic beta cells. *Genes Cells* 2004, 9: 261–270.
26. Rutkevich LA and Williams DB. Vitamin K epoxide reductase contributes to protein disulfide formation and redox homeostasis within the endoplasmic reticulum. *Mol Biol Cell* 2012, 23: 2017–2027.
27. Sevier CS and Kaiser CA. Ero1 and redox homeostasis in the endoplasmic reticulum. *Biochim Biophys Acta* 2008, 1783: 549–556.
28. Tavender TJ and Bulleid NJ. Molecular mechanisms regulating oxidative activity of the Ero1 family in the endoplasmic reticulum. *Antioxid Redox Signal* 2010, 13: 1177–1187.
29. Cain K, Peters S, Hailu H, Sweeney B, Stephens P, Heads J and Sarkar K, *et al.* A CHO cell line engineered to express XBP1 and ERO1-L $\alpha$  has increased levels of transient protein expression. *Biotechnol Prog* 2013, 29: 697–706.
30. Onda Y, Kumamaru T and Kawagoe Y. ER membrane-localized oxidoreductase Ero1 is required for disulfide bond formation in the rice endosperm. *Proc Natl Acad Sci USA* 2009, 106: 14156–14161.